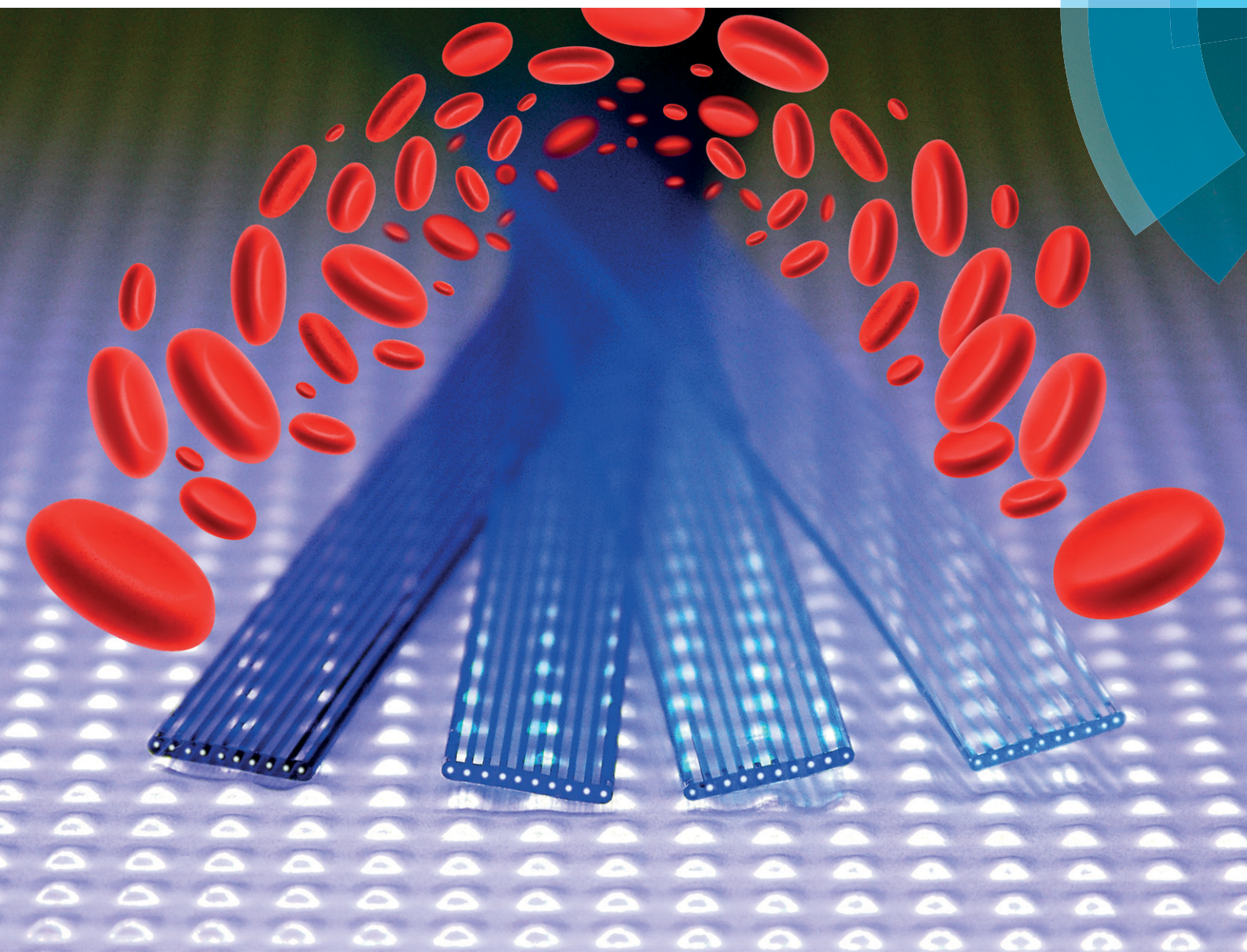


# Lab on a Chip

Miniaturisation for chemistry, physics, biology, materials science and bioengineering  
[www.rsc.org/loc](http://www.rsc.org/loc)



ISSN 1473-0197



PAPER

Nuno M. Reis *et al.*

A lab-in-a-briefcase for rapid prostate specific antigen (PSA) screening from whole blood

Cite this: *Lab Chip*, 2014, **14**, 2918

## A lab-in-a-briefcase for rapid prostate specific antigen (PSA) screening from whole blood†

Ana I. Barbosa,<sup>a</sup> Ana P. Castanheira,<sup>b</sup> Alexander D. Edwards<sup>bc</sup> and Nuno M. Reis<sup>\*ab</sup>

We present a new concept for rapid and fully portable prostate specific antigen (PSA) measurements, termed “lab-in-a-briefcase”, which integrates an affordable microfluidic ELISA platform utilising a melt-extruded fluoropolymer microcapillary film (MCF) containing an array of 10 200  $\mu\text{m}$  internal diameter capillaries, a disposable multi-syringe aspirator (MSA), a sample tray pre-loaded with all of the required immunoassay reagents, and a portable film scanner for colorimetric signal digital quantification. Each MSA can perform 10 replicate microfluidic immunoassays on 8 samples, allowing 80 measurements to be made in less than 15 minutes based on semi-automated operation, without the need of additional fluid handling equipment. The assay was optimised for the measurement of a clinically relevant range of PSA of 0.9 to 60.0  $\text{ng ml}^{-1}$  in 15 minutes with CVs on the order of 5% based on intra-assay variability when read using a consumer flatbed film scanner. The PSA assay performance in the MSA remained robust in undiluted or 1:2 diluted human serum or whole blood, and the matrix effect could simply be overcome by extending sample incubation times. The PSA “lab-in-a-briefcase” is particularly suited to a low-resource health setting, where diagnostic labs and automated immunoassay systems are not accessible, by allowing PSA measurement outside the laboratory using affordable equipment.

Received 18th April 2014,  
Accepted 9th June 2014

DOI: 10.1039/c4lc00464g

[www.rsc.org/loc](http://www.rsc.org/loc)

## Introduction

Prostate cancer is the second most common cause of cancer and the sixth leading cause of death by cancer among the male population worldwide.<sup>1</sup> Currently, prostate specific antigen (PSA) is the most reliable tumor biomarker for prostate cancer diagnosis and for monitoring disease recurrence after treatment.<sup>2</sup> The highest prostate cancer incidence rates have been estimated to occur in the highest resource areas of the world; however, higher mortality rates are seen in low- to medium-resource areas of South America, the Caribbean, and sub-Saharan Africa.<sup>1</sup> Two possible reasons for high mortality rates in low resource settings are the lack of early detection and the absence of appropriate diagnostic testing alongside limited treatment options.

PSA serum concentration in healthy males is in the range of 0–4  $\text{ng ml}^{-1}$  and increases in men with prostate cancer.<sup>3</sup>

Several studies of screened populations showed that individuals with PSA levels in the range of 4–10  $\text{ng ml}^{-1}$  had a 22–27% likelihood of developing cancer, with those with PSA levels of  $\geq 10 \text{ ng ml}^{-1}$  having a risk increasing to 67%.<sup>4–7</sup> The Food and Drug Administration (FDA) approved the determination of PSA serum levels to test asymptomatic men for prostate cancer, in conjunction with digital rectal exam (DRE), in men aged 50 years old or older with a cut-off blood PSA value of 4  $\text{ng ml}^{-1}$ .<sup>8,9</sup> However, some organizations and studies advise undergoing periodic PSA screening from the age of 40 for African American men and men with a family history of prostate cancer.<sup>10</sup> After diagnosis and treatment of primary disease, regular PSA measurements are also routinely used to monitor disease progression and inform clinical decision making. Prostate cancer recurrence is investigated when the PSA blood levels reach 0.4  $\text{ng ml}^{-1}$  in patients with radical prostatectomy<sup>11–15</sup> and 2  $\text{ng ml}^{-1}$  above the post-treatment PSA nadir (the absolute lowest level of PSA after treatment) for patients submitted to radiotherapy.<sup>13,16</sup> Although the efficacy of cancer screening programs is generally complex, recent studies have suggested that PSA screening may decrease prostate cancer mortality.<sup>17–20</sup>

PSA levels are commonly quantified in blood samples in laboratories by sandwich enzyme-linked immunosorbent assay (ELISA). The microtiter plate (MTP) remains a common platform for ELISA in diagnostic laboratories, offering several advantages including established methods and a wide range of reagents and kits alongside wide availability of plate readers,

<sup>a</sup> Department of Chemical Engineering, Loughborough University, Loughborough LE11 3TU, UK. E-mail: [n.m.reis@lboro.ac.uk](mailto:n.m.reis@lboro.ac.uk); Fax: +44 (0)1509 223 923; Tel: +44 (0)1509 222 505

<sup>b</sup> Capillary Film Technology Ltd, Daux Road, Billingshurst, West Sussex, RH14 9SJ, UK

<sup>c</sup> Reading School of Pharmacy, Whiteknights, PO Box 224, Reading, RG66AD, UK. E-mail: [a.d.edwards@reading.ac.uk](mailto:a.d.edwards@reading.ac.uk); Fax: +44 (0)118 931 4404;

Tel: +44 (0)118 378 4253

† Electronic supplementary information (ESI) available. See DOI: [10.1039/c4lc00464g](https://doi.org/10.1039/c4lc00464g)



automated plate handling instruments and plate washers. MTP-based ELISA is highly quantitative and sensitive enough to reach a low limit of detection (LoD) at the picomolar range.<sup>21</sup> However, MTP ELISA cannot be performed outside the laboratory, requires long incubation times and must be performed by trained personnel. These limit the suitability of MTP for the ever increasing demand for measurement of biomarkers such as PSA<sup>22,23</sup> and prevent PSA screening or monitoring in low resource areas where diagnostic laboratories have limited capacity.<sup>24</sup> A rapid, inexpensive, portable and quantitative ELISA platform is therefore urgently required for both high and low resource health systems in order to simplify PSA screening and monitoring. This should integrate simple manual fluid handling with a simple signal measurement system and avoid the need for expensive instrumentation.

One approach to point-of-care PSA quantification is to develop a fully quantitative lateral flow assay, for example, by using fluorescence detection<sup>25</sup> or by scanning the band intensity of colorimetric lateral flow strips.<sup>26</sup> Although lateral flow assays have the assay speed, simplicity, low cost and portability appropriate for point-of-care diagnostics, the suitability for quantitative applications remains unclear, and thus they remain most suited to qualitative diagnostic tests.<sup>27</sup> Lateral flow systems also lack the capacity to perform multiple replicate tests in a single assay, preventing the use of internal standard reference assays alongside the sample.

Recently microfluidic devices have overcome several limitations of the MTP for performing ELISA by capturing the analyte on the surface of a microchannel or using particles entrapped inside the microchannels to increase the surface-to-volume ratio and reduce diffusion distances, resulting in greatly reduced assay times.<sup>28</sup> Many microfluidic immunoassay systems have been reported for the detection of a wide range of analytes, including measurement of cancer biomarkers such as PSA.<sup>29–33</sup> The major remaining challenges for microfluidic devices include controlling fluid flow and developing simple inexpensive detection systems. For example, power-free Lab-on-a-Chip PSA measurement in serum was achieved by manually moving magnetic particles through a device using a permanent magnet.<sup>34</sup> Mobile phone cameras were used for colorimetric signal quantification.<sup>34,35</sup> However, the inability of using several replicates in the same run might compromise assay precision, and these devices do not have the capacity for running internal reference samples alongside the sample. A major drawback for most microfluidic devices also remains the high fabrication cost preventing rapid product development from laboratory prototypes.

We propose here a new “lab-in-a-briefcase” concept for rapid, manual, portable and cost-effective PSA screening, based on an affordable miniaturised ELISA platform that utilises a melt-extruded microcapillary film (MCF).<sup>36</sup> We developed a manually operated device capable of performing 80 microfluidic quantitative ELISA tests in <15 minutes and read using a flatbed scanner. Standard reference curves and sample replicates are measured simultaneously, allowing

internal assay calibration. The entire system can be carried in a small briefcase, a handbag or a laptop case, and the assay can be performed by a single operator with minimal training and requires no additional equipment or instrumentation. We present here the optimisation and performance data for this new system that demonstrates its ability to measure clinically relevant PSA concentrations in human serum and whole blood over a range of operating temperatures. This portable microfluidic system has the potential to give large populations access to affordable PSA screening and monitoring.

## Materials and methods

### Reagents and materials

A human kallikrein 3/prostate specific antigen (PSA) ELISA kit was purchased from R&D Systems (Minneapolis, USA; cat. no. DY1344). The kit contained a monoclonal mouse human kallikrein 3/PSA antibody (capture antibody), a human kallikrein 3/PSA polyclonal biotinylated antibody (detection antibody) and a recombinant human kallikrein 3/PSA (standard). ExtrAvidin-Peroxidase (cat. no. E2886), SIGMAFAST™ OPD (*o*-phenylenediamine dihydrochloride) tablets (cat. no. P9187), *o*-phenylenediamine dihydrochloride (cat. no. P1526-25G), urea hydrogen peroxide (cat. no. 289132), and phosphate–citrate buffer tablets, pH 5.0 (cat. no. P4809) were sourced from Sigma Aldrich Ltd (Dorset, UK). 3,3',5,5'-Tetramethylbenzidine (TMB) (cat. no. DY999) from R&D Systems was also used as an alternative enzymatic substrate. High Sensitivity Streptavidin-HRP was supplied by Thermo Scientific (Lutterworth, UK; cat. no. 21130) and used for enzyme detection.

Phosphate-buffered saline (PBS, Sigma Aldrich, Dorset, UK; cat. no. P5368-10PAK), pH 7.4, 10 mM was used as immunoassay buffer. The diluent and blocking solution consisted of either SuperBlock (Thermo Fisher Scientific, Loughborough, UK; cat. no. 37515) or 1 to 3% (w/v) protease-free bovine serum albumin (BSA, Sigma Aldrich, Dorset, UK; cat. no. A3858) in PBS buffer. For washings, PBS with 0.05% (v/v) of Tween-20 (Sigma-Aldrich, Dorset, UK; cat no P9416-50ML) was used. Nunc MaxiSorp ELISA 96-well MTPs were sourced from Sigma Aldrich (Dorset, UK). Normal off the clot human serum from a single female post-menopausal donor (product code S1221) was supplied by SunnyLab (Broad Oak Road, Sittingbourne, UK). The whole blood used was obtained from umbilical cord through the NHS England and collected into a bag with citrate phosphate dextrose (CPD) as the anticoagulant.

### “Lab-in-a-briefcase” components

The “lab-in-a-briefcase” (Fig. 1) comprises four components: 1) a set of 15 × 12 × 1 cm<sup>3</sup> disposable multiple syringe aspirator (MSA) devices, each of which can perform 10 replicate ELISA tests on each of the 8 samples; 2) customised microwell plates pre-loaded with reagents that interface with the MSA; 3) a portable USB powered film scanner for colorimetric signal quantification; and 4) a portable computer for real-time data analysis. If required, diluent plus disposable pipettes



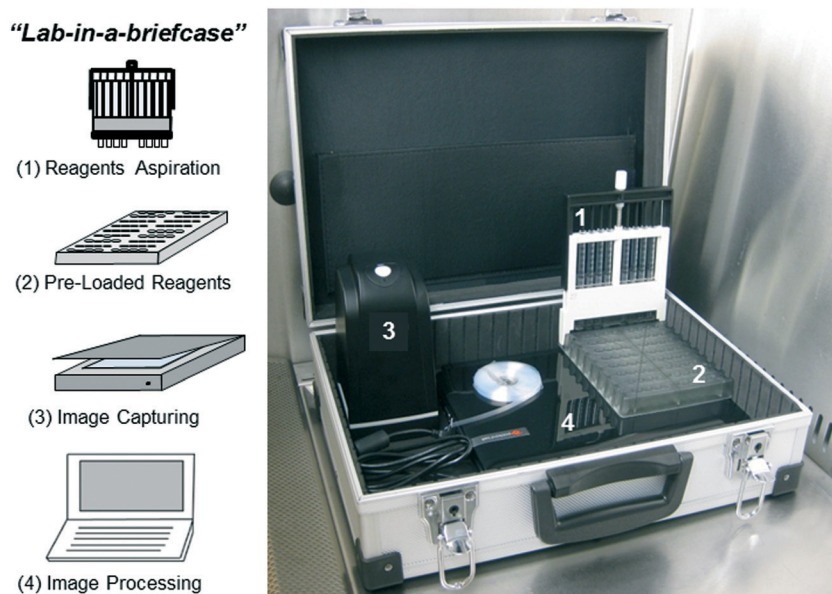


Fig. 1 Main components of “lab-in-a-briefcase” for PSA screening.

can be included for diluting samples to extend the assay's dynamic range. The overall dimensions of this portable lab can be  $40 \times 30 \times 15 \text{ cm}^3$  and it can weigh up to 3 kg, which can be significantly reduced with an alternative detection system, such as a smartphone with an embedded CMOS camera and imaging processing software. Potentially, the detection system can be further miniaturised and made fully disposable using inexpensive electronics containing an LED and photodiodes powered by a small battery similar to existing electronic pregnancy tests.

Each MSA device includes unique design features that minimise the possibility of operator error (e.g. asymmetric edges and a single thumb wheel to control sample and reagent aspiration). Fluid aspiration within the MSA cartridge is driven by 8 plastic, 1 ml syringes driven by a simple thumb wheel and a central threaded rod. Each syringe is connected to a single 30 mm long strip of fluoropolymer MCF containing 10 bore, 200  $\mu\text{m}$  internal diameter microcapillaries pre-coated internally with a monoclonal capture antibody (Fig. S1, ESI<sup>†</sup>). The MSA combines with a customized microwell plate loaded with reference standard samples, assay reagents and wash buffer, plus empty sample wells for clinical samples. One MSA device plus microwell plate can analyse 8 independent samples, allowing the option of comparing a single sample with 7 reference samples or as many as 4 samples with 4 reference samples.

The MCF is a long, continuous plastic film containing a parallel array of microcapillaries (Fig. S1A, ESI<sup>†</sup>) with controlled size and shape resulting from air aspiration/injection through a specially designed melt-extrusion die.<sup>36</sup> The surface characteristics (hydrophobic) and the geometry of the fluoropolymer MCF (flat film) make it a reliable platform for immunoassay techniques, including ELISA.<sup>37</sup> The “lab-in-a-briefcase” uses an MCF ribbon produced from fluorinated

ethylene propylene (FEP-Teflon), containing 10 embedded capillaries with a mean hydraulic diameter of  $206 \pm 12.2 \mu\text{m}$  manufactured by Lamina Dielectrics Ltd (Billingshurst, West Sussex, UK). The external dimensions of the fluoropolymer MCF used in this study were  $4.5 \pm 0.10 \text{ mm}$  wide by  $0.6 \pm 0.05 \text{ mm}$  thick.

The hydrophobicity of MCF fluoropolymer allows the antigen and antibodies to be immobilised on the inner surface of the microcapillaries by passive adsorption.<sup>37</sup> MCF extruded from FEP has exceptional optical transparency because its refractive index<sup>38</sup> of 1.34 to 1.35 matches the refractive index of water (1.33), allowing simple optical detection of colorimetric substrates<sup>37</sup> (Fig. S2, ESI<sup>†</sup>).

#### PSA sandwich ELISA in the fluoropolymer MCF

For each duplicate run using the MSA, the inner surface of the microcapillaries in a 50 cm long fluoropolymer MCF was coated with a human kallikrein 3/PSA capture antibody (CapAb) within a concentration range of  $10\text{--}40 \mu\text{g ml}^{-1}$  in phosphate-buffered saline (PBS). This solution was incubated overnight at 4 °C or for a minimum of 2 hours at room temperature (20 °C). The MCF surface was then blocked using the immunoassay diluents, 1 to 3% BSA-PBS or SuperBlock Solution, for at least 1 hour at room temperature, after which the MCF was washed and trimmed to produce eight 30 mm long fluoropolymer MCF test strips which were inserted into the push-fit seal and then fitted into the MSA. The performance of the assay was found to be not affected when some capillaries lose the washing solution in that process (data not shown). Depending on the required stability, the coated strips can be stored and supplied dried using stabilizing reagents typically developed for MTP-based immunoassays.

Recombinant PSA protein standards loaded into the sample wells of the plate were aspirated into MCF strips in

the MSA cartridge with 6 full revolutions of the central wheel (Fig. S3A, ESI†), and the cartridge was left in the plate with the MCF immersed in samples for incubation. Each wheel rotation draws up 13  $\mu$ l through the MCF test strips, thus 6 turns correspond to 78  $\mu$ l of reagent per 10 bore assay strip. This volume was in great excess compared to the small internal volume of each 30 mm strip (approximately 10  $\mu$ l) to ensure complete solution replacement, which allowed skipping of washing steps in the sandwich immunoassay.

The MSA cassette was then moved to the next row of wells in the MSA plate containing biotinylated detection antibody (DetAb) within the range of 0.5–2  $\mu$ g ml<sup>−1</sup> in PBS. The solution was aspirated with 6 turns of the wheel and incubated for the required time. Subsequently this procedure was repeated for the enzyme conjugate (ExtrAvidin Peroxidase and High Sensitivity Streptavidin-HRP). Finally, the MCF test strips were washed 3 to 4 times with PBS-T (washing buffer) using 6 turns of the thumb wheel per wash (Fig. S3B, ESI†).

The enzymatic substrate (OPD or TMB) was then aspirated into the MCF strips and the MSA containing the MCF strips was laid flat on an HP ScanJet G4050 Film Scanner, and RGB images of 2400 dpi resolution scanned in transmittance mode (Fig. S2B, ESI†) were taken at a given time interval. The MSA provides good alignment of the test strips with the glass surface of the scanner at a distance within the focal distance of the linear CMOS detector (about 6 mm). The volume of the 1 ml disposable syringes was sufficient to deliver homogeneous aspiration of each immunoassay reagent and good washing before the addition of the colorimetric substrate. RGB images of the fluoropolymer test strips array were then taken every 2 to 5 min for up to 30 minutes and analysed using ImageJ (NIH, USA) to quantify absorbance in each individual capillary (Fig. S2C, ESI†) from the greyscale pixel intensity. The RGB image was split into red, green and blue channels, and for the OPD substrate the blue channel was used as it provided maximum light absorption, whereas for TMB the red channel showed the highest absorbance.

Assay optimisation studies were done based on an experimental matrix which consisted in analyzing the effect of 7 factors: capAb concentration, detAb concentration, detAb incubation time, PSA incubation time, enzyme concentration, enzyme incubation time, and matrix effect. All factors were optimised based on the maximum signal-to-noise ratio and total assay time (Fig. 4A and S5, ESI†).

Kinetic studies involving optimum incubation times were performed using the optimised concentrations of 40  $\mu$ g ml<sup>−1</sup> capAb, 1  $\mu$ g ml<sup>−1</sup> detAb, 1  $\mu$ g ml<sup>−1</sup> high sensitivity streptavidin, and 4 mg ml<sup>−1</sup> *o*-phenylenediamine dihydrochloride (OPD) with 1 mg ml<sup>−1</sup> hydrogen peroxide.

The matrix effect was studied after the assay optimisation process (Fig. 4A). It was tested by performing in parallel three different PSA full response curves, one with a buffer solution spiked with diluted concentrations of recombinant proteins (0% serum) and the others by diluting the PSA standards in 100% and 50% (in PBS) female serum within a total assay time of  $\leq$ 15 minutes. To complement the study of the sample

matrix on PSA sandwich assay, other sets of experiments where PSA standards were spiked in non-diluted serum and whole blood matrices were performed. Resulting absorbance values were compared to absorbance values of PSA standards diluted in buffer. To finalize the matrix effect studies, the sample incubation time was increased to  $\geq$ 10 minutes and two PSA assays were performed in parallel, one in buffer (0% serum) and the other in non-diluted serum (100% serum) in a total assay time of  $\sim$ 30 minutes. For the purpose of this comparison, the assay conditions were 10  $\mu$ g ml<sup>−1</sup> capAb incubated overnight at 4 °C, 2  $\mu$ g ml<sup>−1</sup> detAb incubated for 10 minutes, 4  $\mu$ g ml<sup>−1</sup> ExtrAvidin Peroxidase incubated for 10 minutes, and 4 mg ml<sup>−1</sup> *o*-phenylenediamine dihydrochloride (OPD) with 1 mg ml<sup>−1</sup> hydrogen peroxide incubated for 3 minutes.

The 4-parameter logistic (4PL) mathematical model was fitted to the experimental data by the minimum square difference for each full PSA response curve. The lower limit of detection (LoD) was calculated by the mean absorbance of the blank plus three times the standard deviation of the blank samples.

### Measurement of absorbance, absorbance ratio and intra-assay variability in MCF strips

The absorbance (Abs) in the MCF strips was measured from the greyscale pixel intensity of scanned images using image analysis. This consisted of running a profile plot across the greyscale images of the MCF strips (blue channel) and measuring the baseline greyscale pixel intensity across each strip ( $I_0$ ) and the peak height ( $I$ ) at the center of each capillary, where Abs could be directly determined:

$$\text{Abs} = -\log(I/I_0) \quad (1)$$

This procedure was repeated for each individual capillary on each separate MCF strip. Response curves for PSA performed in the MCF strips were compared to those performed in the MTP by considering a mean light path distance of 200  $\mu$ m for each capillary in the MCF strips.

In order to understand signal variability across the different microcapillaries within the same MCF strip (intra-assay variability), MCF strips were immersed in liquid nitrogen, sliced with a razor blade and observed using a long distance microscope (Nikon SMZ1500). The mean hydraulic diameter and the width ( $w$ ) and height ( $h$ ) of each capillary (Fig. 2) were then measured using ImageJ. For each strip, at least 10 slices were analysed at 30 mm intervals which corresponds to the distance of the pre-coated MCF strips required to operate the MSA.

In parallel, MCF strips from the same batch were filled with a 1:2 dilution series of 2 mg ml<sup>−1</sup> 2,3-diaminophenazine (DAP), the colored product resulting from the enzymatic conversion of the chromogenic OPD substrate. The MCF strips were then scanned using the same film scanner and absorbance values determined by image analysis using ImageJ.



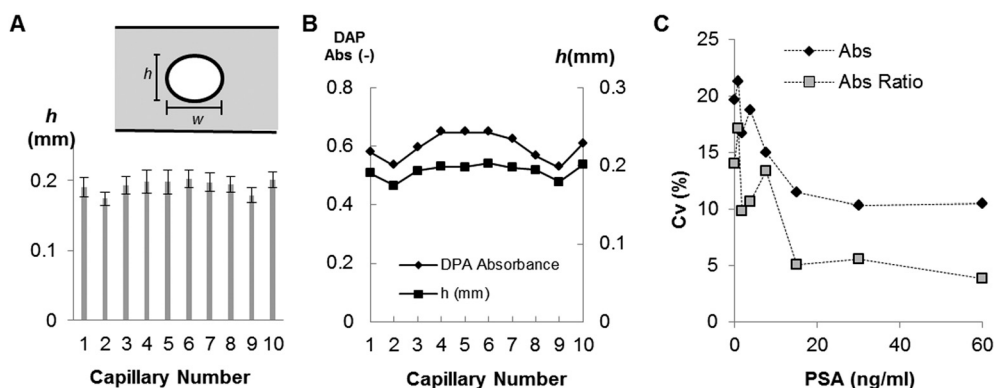


**Fig. 2** Correlation between capillary height ( $h$ ) and absorbance (Abs) variability across a 10 bore fluoropolymer MCF material. A) Variation in  $h$  across and along the MCF strip (error bars represent 2 standard deviations from multiple measurements along a 1 m long MCF strip). B) Correlation between  $h$  and DAP absorbance. C) Coefficient of variation (CV) of absorbance values for different PSA concentrations before and after normalisation with DAP absorbance; CV is obtained from the ratio between the relative standard deviation (STDEV) absorbances along 10 capillaries for a given PSA concentration and the mean value of absorbance in the same 10 capillaries.

This allowed normalizing Abs values with respect to the DAP reference solution, which was expressed in this paper as absorbance ratio (Abs ratio) values:

$$\text{Abs ratio} = \frac{\text{Abs}_{\text{PSA}}}{\text{Abs}_{\text{DAP}}} \quad (2)$$

#### Robustness studies for PSA sandwich ELISA in the MCF

The effect of temperature on the PSA assay performance was tested by running full response curves using the optimised PSA protocol and all reagents were brought to an operating temperature of 4, 20 or 37 °C.

The intra-assay variability studies were accomplished by measuring the absorbance of the lower, middle and upper range of PSA values (3.75, 7.5 and 30 ng ml<sup>-1</sup> PSA) in the 10 capillaries of one MCF strip. These values were already normalized by DAP absorbance, which means that the variability obtained is only intrinsic to the assay and does not depend on the platform geometry variation.

The inter-assay variability was determined by performing PSA assay in the MCF for three PSA concentrations: 3.75, 7.5 and 30 ng ml<sup>-1</sup> (lower, middle and higher range) in three different days and using different MSA devices. The absorbance was measured for 20 samples ( $n = 20$ ) of each PSA concentration studied. For every PSA concentration the inter-assay variability was obtained by calculating the coefficient of variation (CV) between the absorbance of 3 independent PSA sandwich assay runs.

#### PSA sandwich ELISA in 96-well MTP

The protocol recommended by the ELISA kit manufacturer was followed for PSA assay detection in a 96-well MTP which is summarized in Table S1.† The OPD was added to each well and slightly mixed and the absorbance was measured at 450 nm using the Epoch (BioTek) microplate reader. In this instance no stop solution was used in order to compare directly the colorimetric data obtained in the MCF strips with

data from the flatbed film scanner. Absorbance values were expressed as cm<sup>-1</sup> based on a light path length of 0.30 cm for a 96-well microtiter plate.

## Results and discussion

#### Optimisation of the manual and portable lab-in-a-briefcase ELISA

The inexpensive microengineered MCF material was first presented as a miniaturised immunoassay platform for low cost microfluidic direct ELISA,<sup>37</sup> but the majority of immunoassays require a sandwich format including an immobilised capture antibody. To demonstrate the potential of the melt-extruded microfluidic material MCF for delivering affordable, sensitive, clinical testing using a sandwich protocol, we developed a complete ELISA system that shares many benefits with MTP assays but in a portable kit requiring no additional equipment or any complex fluid handling. The core of this system is a manually driven multi-syringe device, termed MSA, combined with a customized microwell plate, that together aspirate samples and all of the required reagents sequentially through MCF strips to perform a full sandwich ELISA (Fig. 1, S1 and S3).† The different geometry, size, and surface-to-area ratio of MCF lead to significant differences under optimum ELISA assay conditions when compared to MTP assays, specifically higher reagent concentrations combined with shorter incubation times. Initial studies therefore focused on identifying the optimum assay conditions for the required sensitivity and for fast total assay times (Fig. S5†).

#### Effect of MCF dimensions on the assay signal

Having established the optimum assay conditions, the next focus was on understanding assay variability. One of the main challenges in microfluidic immunoassays is to maintain the sensitivity and precision of gold standard MTP methodology whilst achieving a major reduction in total assay times. The cost-effective continuous melt extrusion process used to produce MCFs offers the potential for a low-cost device

but has the potential for small variation in the shape and diameter of the microcapillaries along the plastic film and across each film strip. The extent of variation and effect of variations in the geometry of microcapillaries on assay performance have not previously been reported and were studied here by measuring MCF geometry both directly and indirectly using imaging dye solutions within MCF strips.

Based on Lambert-Beer law,  $\text{Abs}$  is linked to the extinction coefficient of a substance ( $\epsilon$ ), concentration ( $c$ ) and light path distance ( $l$ ). Small differences in the shape or size of microcapillaries will therefore affect absorbance independently of the assay signal if the path distance  $l$  changes (Fig. S2†), which could increase assay variability from capillary to capillary across a single MCF strip or between strips taken from film batches with variable dimensions. Initially, the mean hydraulic diameter and capillary height  $h$  of each capillary were measured using an optical microscope in 10 replicate thin samples cut from MCF strips (Fig. 2A). The difference in the internal diameter of each capillary is intrinsic to the melt-extrusion process used for manufacturing the MCF material and typically remains within  $\pm 5\%$ . Although informative, this was a difficult and laborious task because the fluoropolymer MCF was soft and could be deformed during sample slicing, potentially increasing the variability of measured geometry. A second non-invasive method to measure variation in capillary geometry was therefore developed whereby MCF strips were filled with solutions of fixed concentrations of DAP, the coloured product resulting from HRP enzymatic conversion of the chromogenic OPD substrate, and scanned using the same settings as in PSA strips. From the known extinction coefficient of these solutions, variation in capillary height  $h$  could therefore be measured from the  $\text{Abs}$  values calculated from the scanned images. As expected, when measured capillary height was compared to absorbance, a correlation between  $\text{Abs}$  values for DAP was seen with  $h$  (Fig. 2B). When a single DAP reference strip was used to provide reference absorbance and a normalized absorbance ratio was calculated (using eqn (2)), the effect of small differences in the path length distance on PSA assay absorbance was eliminated, resulting in a significant decrease on intra-assay variability over the entire concentration range (Fig. 2C).

### Kinetics of ELISA in MCF capillaries

Quantitative heterogeneous immunoassays usually require extended incubation times to attain the antibody-antigen binding equilibrium. These are dependent on the reagent mass transfer and kinetic limitations.<sup>39</sup> The long incubation times required for sandwich PSA immunoassay in the MTP are linked to the long diffusion distances in the plastic wells that can be dramatically reduced in a miniaturised system. Kinetic studies for each core sandwich ELISA step in the fluoropolymer MCF after assay optimisation confirmed the very short times required to achieve full signal response in a system with a diffusion distance 15 times shorter. An incubation time of 2 min for recombinant protein was found

sufficient in the MCF, whereas for DetAb and the enzyme conjugate no benefit was seen in extending incubation times beyond 5 min (Fig. 3). With respect to the enzymatic chromogenic substrate (OPD), incubation times of up to 10 min followed a zero order reaction (Fig. 3iii; data not shown) which is ideal for obtaining a broad dynamic range in immunoassays, as an early reading can provide good assay performance for higher concentrations; in contrast, low concentrations with weak initial signals can be more clearly measured. As expected for enzyme assays, measurement of the reaction rate rather than endpoint absorbance can also provide a good indication of sample concentration.

Many microfluidic platforms reported successful quantification of biomarkers over a certain dynamic range with total

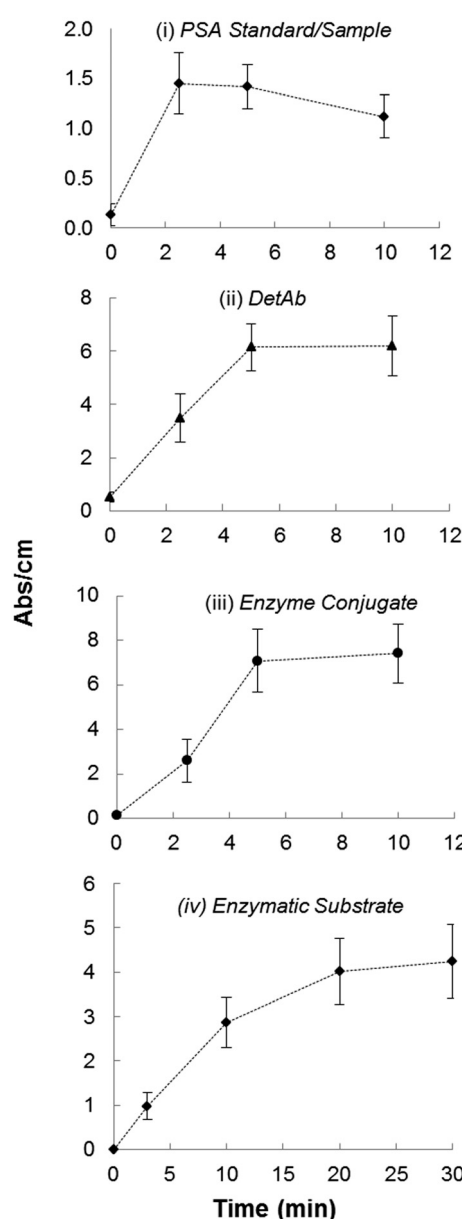


Fig. 3 Kinetics of all assay steps illustrating minimum incubation times required for signal saturation with  $3.75 \text{ ng mL}^{-1}$  PSA recombinant protein.



assay times ranging from 2 minutes to several hours.<sup>40–42</sup> The MCF ELISA can successfully quantify PSA in diluted human serum in 15 minutes, requiring <5 minutes of sample incubation time (Table 1). This total assay time could also be achieved using the Immuno-pillar chip and a capillary driven device using a PDMS substrate, which were able to run human serum sandwich assays presenting similar MCF sensitivity within 12 and 14 minutes of total assay time, respectively.<sup>31,43</sup> Although time competitive, these devices are tailored to single sample and single test, in contrast to the independent 8 samples measured 10 times each in the MSA. In addition, these microfluidic devices use fluorescence microscopes for signal detection, which allow the high sensitivity of the assays but also increase the cost and difficulties for the platform operator, characteristics not suitable for POC applications. Colorimetric detection by a flatbed scanner or other portable devices (*e.g.* smartphone camera) is ideal for POC settings. It is an easy-to-use, portable, user-friendly, rapid and cost effective detection strategy.<sup>28,44</sup> So far, no other microfluidic platform has reported a fully quantitative sandwich immunoassay in  $\leq 15$  minutes using biological samples and colorimetric detection by a flatbed scanner. The new platform can be further miniaturised and turned fully disposable using inexpensive electronics containing a LED and photodiodes powered by a small battery, similar to existing electronic pregnancy tests.

### Assay performance with biological samples

Immunoassay performance can often be affected when human samples are tested with a high and variable concentration of unrelated proteins, lipids, and other biomolecules plus changes in viscosity often producing unwanted background or loss in signal.<sup>45–47</sup> Identifying these interferences and managing them are fundamental for sensitive and reproducible immunoassays.<sup>47</sup> Managing matrix effects becomes even more urgent in POC settings, where the sample processing needs to be minimized or eliminated to speed up the testing process.<sup>44</sup>

After PSA assay optimisation (Fig. 4A) the PSA assay was tested with 100% human serum. The full PSA response curve obtained presented a loss in absolute absorbance signal without a significant loss in sensitivity compared to buffer (Fig. 4B and Table 2). This observation showed however that the biological matrix was interfering with the assay. A further set of experiments compared the performance in 100% human

serum with 100% anticoagulated whole blood as sample matrix for the PSA standards. The results showed that the absorbance values are similar for serum and for whole blood but still lower than those performed in buffer for different concentrations (Fig. 4C). These observations confirm that the PSA MCF assay presents the same performance in serum and in blood, simplifying the sample preparation process by eliminating the need for sample preparation. To our knowledge this finds no precedent in microfluidic devices. Two methods were used to avoid the observed matrix interference. Firstly, 1:2 diluted human serum or blood for full response curves of the PSA MCF sandwich assay was tested, as reported in other microfluidic immunoassay studies.<sup>48</sup> When the absolute Abs values and sensitivity of PSA assay in buffer, diluted serum and diluted blood were compared, similar values were obtained with 15 minutes of total assay time (Fig. 4D). This means that sample dilution can be used to overcome the matrix effect.<sup>48,49</sup> The second method used to overcome the matrix effect consisted in simply increasing the sample incubation times so that the PSA protein (MW 26 kDa<sup>50</sup>) would have time to diffuse through the viscous matrix and bind to the immobilized antibody on the capillary walls. These experiments performed in 100% serum showed that with 15 minutes of sample incubation no difference was noticed between the PSA absorbance values in buffer and in non-diluted serum (Fig. 4E). These results suggest that the matrix effect in the PSA MCF system is due to increased viscosity in the sample and not to the presence of specific interference by proteins or other components of the matrix.<sup>45</sup> At 20 °C the viscosity of buffer is approximately 1 mPa s, whilst the viscosity of serum is known to be higher.<sup>51</sup> The diffusion coefficient of a spherical particle through a liquid with low Reynolds number is directly proportional to diffusion time and inversely proportional to viscosity. This can justify the need for higher sample incubation times for assays performed in non-diluted biological samples and the same absorbance values for 1:2 diluted serum samples with 2-minute sample incubation. Therefore to overcome the viscosity effect of non-diluted samples an extended sample incubation time should be considered, otherwise the sample would need to be diluted 1:2 to match the viscosity to that of the buffer. The absorbance values of the PSA assay in whole blood were similar to those in non-diluted serum, despite blood viscosity being reported to be between 3.36 and 5.46 mPa s.<sup>51</sup> The higher viscosity of blood compared to serum relates to the viscoelastic properties of red blood cells, which appears to not interfere with protein diffusion in the liquid matrix (*i.e.* blood serum). Consequently, whole blood samples can be used in the PSA sandwich ELISA in the MCF platform as long as a minimum of 10 minutes of sample incubation is undertaken or the blood sample is diluted 1:2. Overall, the PSA assay in the MCF was fully quantitative at the current clinical range ( $>4$  ng ml<sup>-1</sup>),<sup>52,53</sup> and at lower proposed ranges (2.6 to 4 ng ml<sup>-1</sup>) (Fig. 4 and Table 2),<sup>9,54</sup> presenting a LoD below 0.9 ng ml<sup>-1</sup> of recombinant protein (Table 2) with a precision varying from 3 to 9% based on the intra-assay variability in buffer

**Table 1** Incubation times of ELISA reagents in the standard microtiter plate (MTP) and in the novel microcapillary film (MCF)

Assay step	Time (min)	
	MTP	MCF
PSA incubation	120	2
DetAb incubation	120	5
Enzyme incubation	20	5
Enzymatic substrate incubation	20–30	1.5–3
Total	280	13.5–15



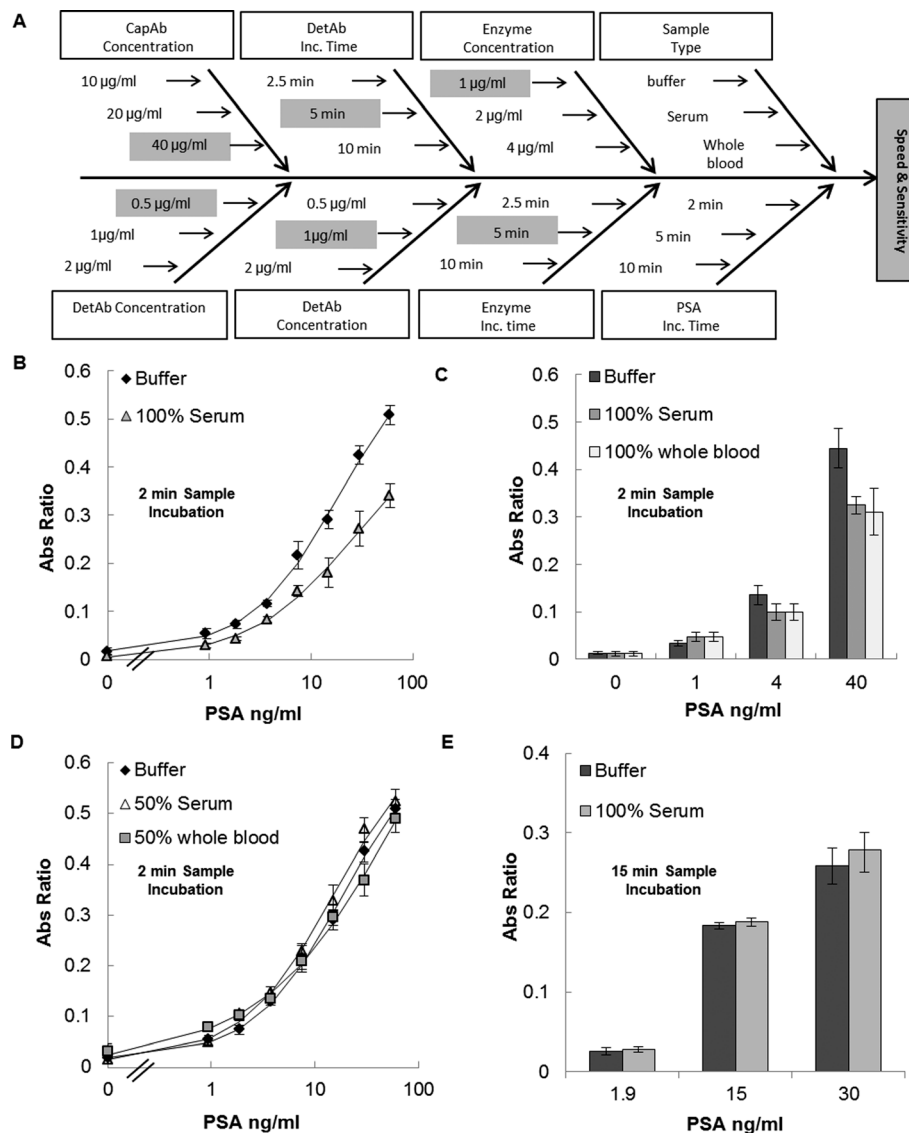


**Fig. 4** PSA sandwich ELISA in the MCF platform using the MSA device. A) Optimisation process and selected experimental conditions. B) MCF PSA assay response curves in 0% and 100% human female serum, spiked with recombinant protein using a total assay time of 15 minutes. C) PSA sandwich assay in buffer, non-diluted serum and whole blood in 15 minutes total assay time (2 minutes sample incubation time). D) MCF PSA assay response curves in 0 and 50% human female serum and 50% human whole blood spiked with recombinant protein in 15 minutes total assay time (2 minutes sample incubation time). E) PSA sandwich assay in 0 and 100% buffer in ~30 minutes total assay time (15 minutes sample incubation).

**Table 2** Parameters of the fully-optimised response curves in the MCF using the MSA device

Assay parameter	Buffer	50% Serum	50% Whole blood	100% Serum
Dynamic range	0.9–60.0 ng ml <sup>-1</sup> ( $R^2 = 0.9988$ )	0.9–60.0 ng ml <sup>-1</sup> ( $R^2 = 0.9981$ )	0.9–60.0 ng ml <sup>-1</sup> ( $R^2 = 0.9983$ )	0.9–60.0 ng ml <sup>-1</sup> ( $R^2 = 0.9988$ )
Sensitivity (LoD)	<0.9 ng ml <sup>-1</sup>			
Precision	5% at 3.8 ng ml <sup>-1</sup>	9% at 3.8 ng ml <sup>-1</sup>	7% at 3.8 ng ml <sup>-1</sup>	7% at 3.8 ng ml <sup>-1</sup>

and in biological samples. The LoD was calculated by adding 3 times the blank standard deviation to the mean blank absorbance; the absorbance value obtained was transformed in a PSA concentration using the 4PL mathematical model. The cross-correlation coefficient  $R^2$  between the 4PL model and the experimental data is also shown in Table 2.

Given that variation in capillary geometry across the MCF strip has already been identified as a significant component

of assay variance (Fig. 2C), it was possible to reduce assay variability by normalizing absorbance values. This was done by dividing each capillary absorbance by the average of absorbance of a reference solution of the DAP strip in the same capillary number, obtaining an absorbance ratio (Fig. 4).

Once the optimised conditions were established for the MCF (Fig. 4A), full PSA response curves were obtained and compared to a 96-well microtiter plate. Performance of the

two platforms was comparable (Fig. S4†) despite the >94% reduction in assay time in the MCF platform (Table 1). A major difference between assays in the MCF and the MTP is that the former requires only one washing step (before addition of the enzymatic substrate), while the MTP involved several washings after each incubation step. The assay sensitivity in the MCF was not affected by the removal of washing

steps, which reduced the total number of steps required, bringing sandwich immunoassays closer to point-of-care devices. The normalized Abs/cm signal in the MTP (Fig. S4†) was almost 50-fold lower than that in the MCF platform using the optimised immunoassay conditions, a reflection of the shorter path length of the microcapillary assay and optimised MCF assay conditions.

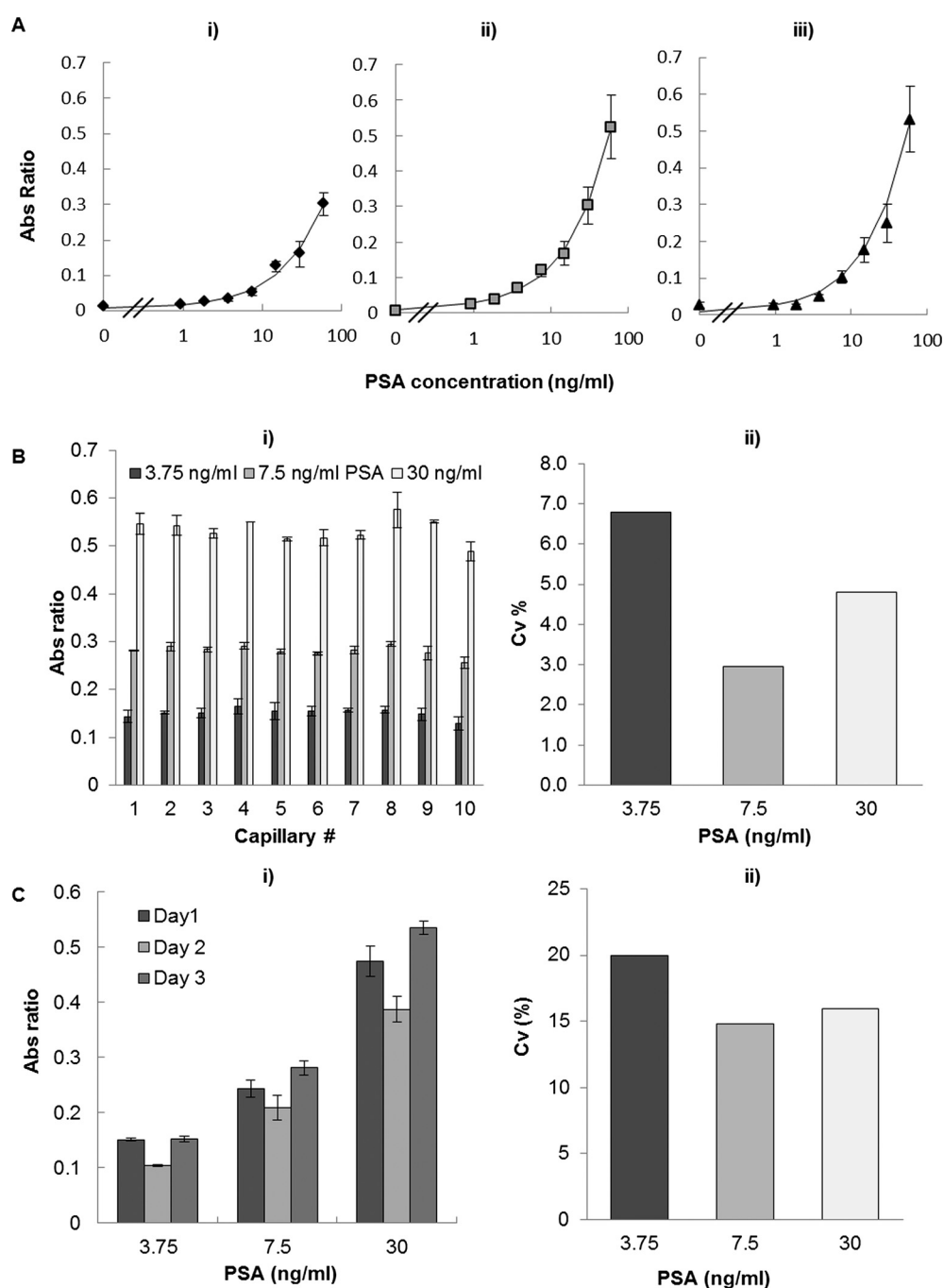


**Fig. 5** Robustness of PSA sandwich assay in the MCF. A) Effect of temperature on the performance of PSA immunoassay in the MCF at i) 4 °C, ii) 20 °C, and iii) 37 °C. B) Intra-assay variability studies at the lower, middle and upper range of the PSA response curve: i) absorbance ratio per capillary and ii) coefficient of variation calculated by the ratio of the standard deviation of 10 absorbance values by the average of those values. C) Inter-assay variability studies at the lower, middle and upper range of PSA assay using different MSA devices: i) inter-assay variability per day and ii) coefficient of variation calculated by the ratio of the standard deviation of 20 absorbance values by the average of those values.



## Robustness of PSA sandwich ELISA in the MCF using MSA devices

Point-of-care testing devices should ideally present robust performance at a range of temperatures, as temperature fluctuations are difficult to control outside the laboratory setting. Temperature has been reported to affect immunoassay performance in terms of linear range, precision and limit of detection.<sup>55,56</sup> A separate set of experiments explored the effect of temperature on PSA sandwich assay performance. Consequently, PSA full response curves were obtained with reagents pre-stabilized at 4, 20 and 37 °C in the MSA with a reduction in the absolute values of absorbance for 4 °C (related to lower HRP enzymatic activity), but limited impact with respect to the LoD or linearity of the PSA immunoassay. In general, temperatures around 20 °C favoured the sensitivity and precision of the assay (Fig. 5A). Similar results were found by Imagawa *et al.*<sup>56</sup> where the lowest non-specific binding and the highest specific binding were obtained by incubation at 20 °C when compared with incubation at 37 °C. Although temperature presents minimum impact on assay performance, the MSA allows performing a full response curve under the same conditions with a given biological sample, therefore providing an internal calibration ideal for POC settings.<sup>44</sup>

A further set of experiments aimed at specifically studying the precision of PSA assay in the MCF at 20 °C. These experiments showed an intra-assay precision of <7% at the lower, middle and upper range of the PSA response curve (Fig. 5B). Note that the 10 samples corresponding to 10 capillaries were analyzed in this process, the CV calculated by the ratio between the standard deviation of Abs values with the absorbance average of the 10 samples. The inter-assay variability was determined by performing the assay in three different days and using three different MSA devices. A total of 20 samples were analysed in order to calculate CV values. The results showed <20% of inter-assay variability (Fig. 5C) which is within the value accepted (25% of variation) for validation of heterogeneous immunoassays according to a pharmaceutical industry perspective.<sup>57</sup> All absorbance values were previously normalized by DAP absorbance, eliminating the effect of capillary geometry variation in the determination of intra- and inter-assay variability.

## Conclusions

We presented a new “lab-in-a-briefcase” concept for sandwich immunoassays employing inexpensive, compact components for point-of-care and field diagnostics detection and demonstrated system performance for the important cancer biomarker PSA (prostate specific antigen) from human serum and whole blood. This portable lab, with dimensions of 40 × 30 × 15 cm<sup>3</sup>, uses a miniaturised ELISA platform, fluoropolymer MCF that offers rapid, low volume and cost-effective assays comparable to MTP ELISA. The flat geometry of the plastic film combined with the optical clarity of the fluoropolymer material provides the opportunity for simple optical detection using USB powered film scanners. A simple and

efficient MSA is used to simultaneously fill 8 pre-coated MCF test strips or 80 capillaries using an array of 1 ml disposable plastic syringes. The components of our portable lab allow the use of conventional ELISA and commercialised assay chemistry in the field outside the laboratory setting. As a proof of concept the PSA ELISA detection using the lab components was performed in 15 minutes in biological samples with a LoD of <0.9 ng ml<sup>-1</sup> PSA and 3 to 10% intra-assay variability. This means that PSA MCF ELISA was 20× faster than the standard MTP ELISA, whilst maintaining similar assay performance with respect to precision and LoD. This has the potential of enabling PSA screening in the patient's home or in remote areas. Future improvement on the “lab-in-a-briefcase” for PSA screening can be achieved by further miniaturising all components or interfacing to wireless, smartphone technology for simple optical signal quantification.

## References

- 1 J. Ferlay, H. Shin, F. Bray, D. Forman, C. Mathers and D. Parkin, *GLOBOCAN 2008*, International Agency for Research on Cancer, Lyon, 2010.
- 2 T. J. Polascik, J. E. Oesterling and A. W. Partin, *J. Urol.*, 1999, 162, 293–306.
- 3 E. D. Crawford, E. P. DeAntoni, R. Etzioni, V. C. Schaefer, R. M. Olson and C. A. Ross, *Urology*, 1996, 47, 863–869.
- 4 M. K. Brawer, J. Beatie, M. H. Wener, R. L. Vessella, S. D. Preston and P. H. Lange, *J. Urol.*, 1993, 150, 106–109.
- 5 M. B. Gretzer and A. W. Partin, *Eur. Urol. Suppl.*, 2002, 1, 21–27.
- 6 M. J. Barry, *N. Engl. J. Med.*, 2001, 344, 1373–1377.
- 7 H.-P. Schmid, W. Riesen and L. Prikler, *Crit. Rev. Oncol. Hematol.*, 2004, 50, 71–78.
- 8 N. C. Institute, <http://www.cancer.gov/cancertopics/factsheet/detection/PSA>, (accessed April 2014).
- 9 G. De Angelis, H. G. Rittenhouse, S. D. Mikolajczyk, L. Blair Shamel and A. Semjonow, *Rev. Venez. Urol.*, 2007, 9, 113–123.
- 10 D. Ulmert, A. M. Cronin, T. Björk, M. F. O'Brien, P. T. Scardino, J. A. Eastham, C. Becker, G. Berglund, A. J. Vickers and H. Lilja, *BMC Med.*, 2008, 6, 6.
- 11 J. K. Parsons, A. W. Partin, B. Trock, D. J. Bruzek, C. Cheli and L. J. Sokoll, *BJU Int.*, 2007, 99, 758–761.
- 12 A. C. Lo, W. J. Morris, V. Lapointe, J. Hamm, M. Keyes, T. Pickles, M. McKenzie and I. Spadinger, *Int. J. Radiat. Oncol., Biol., Phys.*, 2014, 88, 87–93.
- 13 P. C. Albertsen, J. A. Handley, D. F. Penson and J. Fine, *J. Urol.*, 2004, 171, 2221–2225.
- 14 C. L. Amling, E. J. Bergstrahl, M. L. Blute, J. M. Slezak and H. Zincke, *J. Urol.*, 2001, 165, 1146–1151.
- 15 A. J. Stephenson, M. W. Kattan, J. A. Eastham, Z. A. Dotan, F. J. Bianco, H. Lilja and P. T. Scardino, *J. Clin. Oncol.*, 2006, 24, 3973–3978.
- 16 M. K. Buiyounouski, T. Pickles, L. L. Kestin, R. Allison and S. G. Williams, *J. Clin. Oncol.*, 2012, 30, 1857–1863.
- 17 A. V. Fritz, H. Schröder, J. Hugosson and G. Aus, *N. Engl. J. Med.*, 2012, 366, 981–990.

18 G. L. Andriole, J. K. Gohagan and C. D. Berg, *N. Engl. J. Med.*, 2009, **360**, 1310–1319.

19 A. J. Vickers, D. Ulmert, D. D. Sjoberg, C. J. Bennette, T. Bjork, A. Gerdts, J. Manjer, P. M. Nilsson, A. Dahlin, A. Bjartell, P. T. Scardino and H. Lilja, *BMJ*, 2013, **346**, 1–11.

20 S. Loeb and W. J. Catalona, *Cancer Lett.*, 2007, **249**, 30–39.

21 C. Pelaez-Lorenzo, J. C. Diez-Masa, I. Vasallo and M. de Frutos, *J. Agric. Food Chem.*, 2010, **58**, 1664–1671.

22 J. D. Voss and J. M. Schechtman, *J. Gen. Intern. Med.*, 2001, **16**, 831–837.

23 L. Wallner, S. Frencher, J.-W. Hsu, R. Loo, J. Huang, M. Nichol and S. Jacobsen, *Perm. J.*, 2012, **16**, 4–9.

24 M. Ahmed, *Trop. Doct.*, 2011, **41**, 141–143.

25 S. W. Oh, Y. M. Kim, H. J. Kim, S. J. Kim, J.-S. Cho and E. Y. Choi, *Clin. Chim. Acta*, 2009, **406**, 18–22.

26 O. Karim, A. Rao, M. Emberton, D. Cochrane, M. Partridge, P. Edwards, I. Walker and I. Davidson, *Prostate Cancer Prostatic Dis.*, 2007, **10**, 270–273.

27 G. A. Posthuma-Trumpie, J. Korf and A. van Amerongen, *Anal. Bioanal. Chem.*, 2009, **393**, 569–582.

28 C.-C. Lin, J.-H. Wang, H.-W. Wu and G.-B. Lee, *JALA*, 2010, **15**, 253–274.

29 S. Nie, W. H. Henley, S. E. Miller, H. Zhang, K. M. Mayer, P. J. Dennis, E. A. Oblath, J. P. Alarie, Y. Wu, F. G. Oppenheim, F. F. Little, A. Z. Uluer, P. Wang, J. M. Ramsey and D. R. Walt, *Lab Chip*, 2014, **14**, 1087–1098.

30 J. L. Garcia-Cordero and S. J. Maerkli, *Lab Chip*, 2013, DOI: 10.1039/C3LC51153G.

31 M. Ikami, A. Kawakami, M. Kakuta, Y. Okamoto, N. Kaji, M. Tokeshi and Y. Baba, *Lab Chip*, 2010, **10**, 3335–3340.

32 R. S. Sista, A. E. Eckhardt, V. Srinivasan, M. G. Pollack, S. Palanki and V. K. Pamula, *Lab Chip*, 2008, **8**, 2188–2196.

33 J. Kai, A. Puntambekar, N. Santiago, S. H. Lee, D. W. Sehy, V. Moore, J. Han and C. H. Ahn, *Lab Chip*, 2012, **12**, 4257–4262.

34 H. Adel Ahmed and H. M. E. Azzazy, *Biosens. Bioelectron.*, 2013, **49**, 478–484.

35 S. Lee, V. Oncescu, M. Mancuso, S. Mehta and D. Erickson, *Lab Chip*, 2014, **14**, 1437–1442.

36 B. Hallmark, F. Gadala-Maria and M. R. Mackley, *J. Non-Newtonian Fluid Mech.*, 2005, **128**, 83–98.

37 A. D. Edwards, N. M. Reis, N. K. H. Slater and M. R. Mackley, *Lab Chip*, 2011, **11**, 4267–4273.

38 DuPont, [www2.dupont.com/Teflon\\_Industrial/en\\_US/assets/downloads/h55007.pdf](http://www2.dupont.com/Teflon_Industrial/en_US/assets/downloads/h55007.pdf), 1996, (accessed April 2014).

39 W. Kusnezow, Y. V. Syagailo, S. Rüffer, N. Baudenstiel, C. Gauer, J. D. Hoheisel, D. Wild and I. Goychuk, *Mol. Cell. Proteomics*, 2006, **5**, 1681–1696.

40 P. Novo, D. M. F. Prazeres, V. Chu and J. P. Conde, *Lab Chip*, 2011, **11**, 4063–4071.

41 H. C. Tekin and M. A. M. Gijs, *Lab Chip*, 2013, **13**, 4711–4739.

42 R. Gorkin, J. Park, J. Siegrist, M. Amasia, B. S. Lee, J.-M. Park, J. Kim, H. Kim, M. Madou and Y.-K. Cho, *Lab Chip*, 2010, **10**, 1758–1773.

43 L. Gervais and E. Delamarche, *Lab Chip*, 2009, **9**, 3330–3337.

44 P. von Lode, *Clin. Biochem.*, 2005, **38**, 591–606.

45 C. L. Morgan, D. J. Newman, J. M. Burrin and C. P. Price, *J. Immunol. Methods*, 1998, **217**, 51–60.

46 U. Sauer, J. Pultar and C. Preininger, *J. Immunol. Methods*, 2012, **378**, 44–50.

47 M. L. Chiu, W. Lawi, S. T. Snyder, P. K. Wong, J. C. Liao and V. Gau, *JALA*, 2010, **15**, 233–242.

48 M. E. Hoadley and S. J. Hopkins, *J. Immunol. Methods*, 2013, **396**, 157–162.

49 T. P. Taylor, M. G. Janech, E. H. Slate, E. C. Lewis, J. M. Arthur and J. C. Oates, *Biomarker Insights*, 2012, **7**, 1–8.

50 A. Bélanger, H. van Halbeek, H. C. Graves, K. Grandbois, T. A. Stamey, L. Huang, I. Poppe and F. Labrie, *Prostate*, 1995, **27**, 187–197.

51 R. S. Rosenson, A. McCormick and E. F. Uretz, *Clin. Chem.*, 1996, **42**, 1189–1195.

52 A. Caplan and A. Kratz, *Pathol. Patterns Rev.*, 2002, **117**, 104–108.

53 W. J. Catalona, M. A. Hudson, P. T. Scardino, J. P. Richie, F. R. Ahmann, R. C. Flanigan, J. B. DeKernion, T. L. Ratliff, L. R. Kavoussi, B. L. Dalkin, W. B. Waters, M. T. MacFarlane and P. C. Southwick, *J. Urol.*, 1994, **152**, 2037–2042.

54 H. Zhu, K. A. Roehl, J. A. V. Antenor and W. J. Catalona, *Urology*, 2005, **66**, 547–551.

55 J. Grandke, U. Resch-Genger, W. Bremser, L.-A. Garbe and R. J. Schneider, *Anal. Methods*, 2012, **4**, 901.

56 M. Imagawa, S. Yoshitake, S. Hashida and E. Ishikawa, *Anal. Lett.*, 1982, **15**, 1467–1477.

57 J. W. Findlay, W. C. Smith, J. W. Lee, G. D. Nordblom, I. Das, B. S. DeSilva, M. N. Khan and R. R. Bowsher, *J. Pharm. Biomed. Anal.*, 2000, **21**, 1249–1273.

